Available online at www.sciencedirect.com
SCIENCE DIRECT
Earth and Planetary Science Letters 244 (2006) 672–682
EPSL
www.elsevier.com/locate/epsl

Convective mixing of air in firn at four polar sites

Kenji Kawamura [a,b,c,*], Jeffrey P. Severinghaus [c], Shigeyuki Ishidoya [a], Satoshi Sugawara [d], Gen Hashida [e], Hideaki Motoyama [e], Yoshiyuki Fujii [e], Shuji Aoki [a], Takakiyo Nakazawa [a]

[a] *Center for Atmospheric and Oceanic Studies, Graduate School of Science, Tohoku University, Sendai 980-8578, Japan*
[b] *Climate and Environmental Physics, Physics Institute, University of Bern, 3012 Bern, Switzerland*
[c] *Scripps Institution of Oceanography, 9500 Gilman Drive, La Jolla, CA 92093-0244, USA*
[d] *Institute of Earth Science, Miyagi University of Education, Sendai 980-0845, Japan*
[e] *National Institute of Polar Research, Tokyo 173-8515, Japan*

Received 12 October 2005; received in revised form 11 February 2006; accepted 12 February 2006
Available online 22 March 2006
Editor: M.L. Delaney

Abstract

Air withdrawn from the firn at four polar sites (Dome Fuji, H72 and YM85, Antarctica and North GRIP, Greenland) was measured for $\delta^{15}N$ of N_2 and $\delta^{18}O$ of O_2 to test for the presence of convective air mixing in the top part of the firn, known as the "convective zone". Understanding the convective zone and its possible relationship to surface conditions is important for constructing accurate ice-core greenhouse gas chronologies and their phasing with respect to climate change. The thickness of the convective zone was inferred from a regression line with barometric slope of the data in the deep firn. It is less than a few meters at H72 and NGRIP, whereas a substantial convective zone is found at Dome Fuji (8.6±2.6 m) and YM85 (14.0±1.8 m). By matching the outputs of a diffusion model to the data, effective eddy diffusivities required to mix the firn air are found. At the surface of Dome Fuji and YM85, these are found to be several times greater than the molecular diffusivity in free air. The crossover from dominance of convection to molecular diffusion takes place at 7±2, 11±2 and 0.5±0.5 m at Dome Fuji, YM85 and NGRIP, respectively. These depths can be used as an alternative definition of the convective zone thickness. The firn permeability at Dome Fuji is expected to be high because of intense firn metamorphism due to the low accumulation rate and large seasonal air temperature variation at the site. The firn layers in the top several meters are exposed to strong temperature gradients for several decades, leading to large firn grains and depth hoar that enhance permeability. The thick convective zone at YM85 is unexpected because the temperature, accumulation rate and near-surface density are comparable to NGRIP. The strong katabatic wind at YM85 is probably responsible for creating the deep convection. The largest convective zone found in this study is still only half of the current inconsistency implied from the deep ice core gas isotopes and firn densification models.

Keywords: ice core; firn air; convective mixing; wind pumping; glacial cycles; eddy diffusion

1. Introduction

Ice core records of trapped gases have been used extensively to reconstruct the past history of atmospheric greenhouse gases and climate [1–4]. One difficulty

* Corresponding author. Scripps Institution of Oceanography, La Jolla, CA 92093-0244, USA. Tel.: +1 858 822 1642; fax: +1 858 822 3310.
E-mail address: kkawamura@ucsd.edu (K. Kawamura).

0012-821X/$ - see front matter © 2006 Elsevier B.V. All rights reserved.
doi:10.1016/j.epsl.2006.02.017

has been that the trapped gas is younger than the enclosing ice matrix, due to the fact that gas is trapped in bubbles at the base of the ~100-m-thick porous firn layer on top of the glacier [5]. This age difference is not well known for times in the past and thus obscures the phase relationship between changes in greenhouse gases and climate (e.g. [6]). To estimate the ice-age/gas-age difference, knowledge of the past thickness of the firn and accumulation rate are necessary. Glaciological firn densification models are commonly used to predict the firn thickness and thus estimate the age difference, but these models depend strongly on (uncertain) parameters of temperature and accumulation rate [7].

One largely independent check on the models may come from measurements of nitrogen isotopes and other inert gases [6–10]. Gravitational and thermal fractionation in the stagnant part of the firn layer produces a signal in trapped air that is proportional to the firn thickness and top-to-bottom temperature gradient [8,11]. However, air convection near the surface and effective sealing of open pores near the bottom of the firn may obscure the true firn thickness and temperature gradient and thus bias the result, as follows.

The firn is classically divided into three zones with respect to air movement and thus isotopic fractionation [8]. The top 1–20 m from the surface may be the convective zone in which convective mixing overwhelms molecular diffusion and prevents isotopic fractionation. The convection may be induced by pressure gradients due to surface wind [12] or by buoyancy due to seasonal temperature gradients near the surface [13]. The second zone is the diffusive zone, the largest part (40–100 m) of the firn, in which molecular diffusion dominates the gas movement and thus gravitational and thermal fractionation occur. According to the barometric equation, the magnitude of the gravitational fractionation δ_{grav} is approximated by

$$\delta_{\mathrm{grav}} \cong 1000\frac{\Delta mgz}{RT}\,(‰) \qquad (1)$$

where Δm is the mass difference between the isotope pair (kg mol^{-1}), g is acceleration of gravity, z is the thickness of the diffusive zone, R is gas constant, and T is temperature (K) [14]. Thermal diffusion concentrates isotopically heavier gases at the colder end, and its magnitude is given by $\Omega(T_1-T_2)$ (‰), where Ω is thermal diffusion sensitivity (‰ K^{-1}), and T_1 and T_2 are temperature at the warm and cold ends of the diffusive zone, respectively [13]. For modern firn, the vertical gradient of annual mean temperature is small so that thermal fractionation is negligible in comparison with gravitational fractionation. Note however that, in the shallow firn (<~10 m), thermal fractionation is important for the isotopic profile because of seasonal temperature gradients in upper several meters of the firn [13]. The third zone occurs in the bottom 2–12 m and is the lock-in zone (also called non-diffusive zone), in which horizontally extensive high-density layers become ice and thus impermeable. The air exists in open pores between the ice layers, but exchange with neighboring layers is negligibly small (i.e. the air is "locked-in"). The isotopic ratios at the top of the lock-in zone are thus conserved in this zone while the bulk air descends at the same rate as the firn and gradually transforms into air bubbles in the ice. The thickness of the lock-in zone is generally dependent on the magnitude and lateral continuity of layering created at the surface, typically by seasonal variations of snow density.

Air trapped in ice in the Antarctic interior (Vostok, Dome Fuji, Dome C) during glacial periods has shown unexpectedly low gravitational fractionation, as inferred from δ^{15}N and δ^{40}Ar measurements [6]. The deduced thickness of the diffusive zone using Eq. (1) is thinner by up to 30–40 m than the total firn thickness estimated from glaciological firn densification models [6,8,9,15,16]. The discrepancy might be due to a thickened convective zone. However, currently there is no way to estimate past convective zone thickness. In fact, even modern convective zones have been poorly documented due to poor data quality and the actual lack of a substantial convective zone at most studied sites. A significant convective zone has been reported thus far only at one site, Vostok (13 m) ([17]; see [16] for a summary of previous firn studies). It is thus important to quantify the extent of convective zones and to find out what meteorological or glaciological conditions might control their occurrence.

Here we present firn δ^{15}N and δ^{18}O profiles at three Antarctic sites and one Greenland site with varying surface conditions. δ^{18}O is used as an independent measure of the isotopic fractionation in the firn, since the atmospheric δ^{18}O is constant on the decadal timescale. The thickness of the convective zone at each site is estimated from the data by a classic definition using barometric line fitting [17]. In this method, a line with the barometric slope at the site temperature is fitted to the data in the deep part of the firn. The depth intercept at zero isotopic enrichment gives the thickness of the convective zone. We here propose an alternative definition of the convective zone thickness by parameterization of the magnitude of convective mixing using an eddy diffusion term in a 1-dimensional model of diffusion and advection [13]. The firn air data is used to constrain the eddy diffusivity profile, which is then compared with the molecular diffusivity profile, to test the dominance of

Table 1
Surface conditions at studied sites and thickness of convective zone derived by line fitting and model fitting methods

	H72[a, b]	YM85[a]	Dome Fuji[a, c]	North GRIP[d, e]
Location	69.2°S, 41.1°′E	71.6°′S, 40.6°E	77.3°S, 39.7°E	75.1°N, 42.3°W
Elevation (m)	1241	2246	3810	2917
Sampling period	12–21 Sep. 1998	10–17 Jan. 2002	13–25 Dec. 1998	24 May–6 Jun. 2001
10-m firn temperature (°C)	−20.3	−34	−57.3	−31.1
Pressure (hPa)	857	730	600	691
Accumulation (kg m^{-2} yr^{-1})	310	155	26	175
Surface density (kg m^{-3})	390	430	300	340
Mean wind speed (m s^{-1})	8[f]	12[g]	2	4
Viscosity of air ($\times 10^{-6}$ Pa s)[h]	15.7	15.0	13.8	15.1
Molecular diffusivity of N_2 ($\times 10^{-5}$ m^2 s^{-1})[i]	1.71	1.81	1.82	1.96
Convective zone thickness from line fitting (m)	2.4±3.4	14.0±1.8	8.6±2.6	1.1±2.8
Convective zone thickness from model fitting (m)	–	11±2	7±2	0.5±0.5

[a] [21].
[b] [25].
[c] [4].
[d] [26].
[e] [22].
[f] Value at nearby H21 site (69.1°S, 40.8°E).
[g] Value at nearby YM112 site (71.7°S, 39.3°E).
[h] Calculated with Sutherland Law and firn temperature. $\mu=\mu_0[(T/T_0)^{1.5}(T_0+110)]/(T+110)$, where μ_0 is reference viscosity, T is temperature and T_0 is reference temperature.
[i] [5].

eddy diffusion in the shallow firn. The depth at which the eddy diffusivity equals molecular diffusivity may be considered as the convective zone thickness. The model fitting may give a more rigorous assessment of the convective zone than barometric line fitting, because the model includes all physical processes of gas mixing and fractionation (convective mixing, gravitational fractionation, thermal fractionation, and advection), which may slightly alter the isotopic profile from the barometric slope in the deep firn. The model approach can also detect existence of a small convective zone, which is ambiguous by the line fitting method. The relationship between the convective zone thickness and surface conditions including accumulation rate and wind speed are then discussed.

2. Method

2.1. Firn air sampling and measurement

Firn air was sampled at four polar sites with varying surface conditions (Table 1). The three Antarctic sites are located in Drønning Maud Land in East Antarctica at a coastal site (H72), a middle-elevation plateau site (YM85) and a high plateau site (Dome Fuji). The samplings were made at H72 and Dome Fuji in 1998 and at YM85 in 2002 by the Japanese Antarctic Research Expedition teams, as a part of the Japanese contribution to the International Trans Antarctic Scientific Expedition (ITASE). The North GRIP (NGRIP) sampling was made in 2001 in a Japan/EU joint effort as a part of the NGRIP deep drilling project.

Our sampling device is similar to that developed by Schwander et al. [5]. We used a 3-m-long natural rubber packer to seal the borehole, with a LOA piston pump (GAST, USA) and a nylon tube (O.D. = 12.7 mm, I.D. = 9.6 mm, L = 120 m) for the air sampling. The flow rate was typically 13–15 l/min except for the deepest few meters where the flow rate was lower (1–10 l/min). At H72 and Dome Fuji, 250 l of air was pumped to waste from the firn prior to the sampling to avoid contamination. At NGRIP, CO_2 concentration of the firn air was continuously monitored during wasting. Typically, the CO_2 concentration stabilized within 0.3 ppm in 5 min (corresponding to ~70 l). We found that the descending speed of the drill and packer needed to be lower than 0.5 m/s. If the speed was too fast (>~1 m/s), surface air was apparently pushed into the borehole, and we had to waste ~250 l in such instances. Once the CO_2 concentration stabilized, it did not change even after 700 l of air was withdrawn. At YM85, at least 400 l of air was wasted before the sampling. The firn air was pressurized in a metal flask to ~10 bar except at the last few sampling depths, which had somewhat lower

pressures. The sample flask is a cylindrically shaped stainless steel container with metal bellows valves (Nupro SS-4H) attached at both ends. The volume is 1.5 l for Dome Fuji, H72 and NGRIP and 350 ml for YM85. The total numbers of sampled depths are 14, 25, 12, and 24 at Dome Fuji, YM85, H72 and NGRIP, respectively. Duplicate and triplicate samplings were made at YM85 at 12 depths.

δ^{15}N and δ^{18}O were measured at Tohoku University with mass spectrometers consisting of a Finnigan MAT Delta-S (for Dome Fuji, H72 and NGRIP) and a MAT 252 (for YM85 and some NGRIP samples within 0–59.6 m). Samples are measured relative to our reference air in aluminum cylinders. Reproducibility (one standard deviation) is 0.015‰ and 0.035‰ with the Delta-S, and 0.012‰ and 0.026‰ with the MAT 252 for δ^{15}N and δ^{18}O, respectively. δ^{15}N is corrected for isobaric interference from CO_2 molecules that fragment into CO^+ [18]. δ^{15}N and δ^{18}O values are reported as deviations from the isotopic ratios of surface air at each site, in order to compensate for common fractionation during sampling, storage, and measurement.

The experimental uncertainties are estimated based on replicate samplings or measurements. The pooled standard deviations for replicate samples at YM85 are 0.015‰ and 0.021‰ for δ^{15}N and δ^{18}O, respectively, which are comparable to the internal measurement precision. This indicates that the sampling did not introduce additional uncertainty. For YM85, mean values are reported for the depths where replicate sampling was made. The pooled standard deviations derived from NGRIP values measured with both Delta-S and MAT 252 are 0.015‰ and 0.020‰ for δ^{15}N and δ^{18}O, respectively, and there is no appreciable offset between the values from the two mass spectrometers. Thus, the mean of the values measured with the Delta-S and MAT 252 are reported. The error bars in the results (Fig. 1) represent the estimated 1σ uncertainties, consisting of one standard deviation of single measurements for Dome Fuji, H72 and a part of NGRIP data, and one pooled standard deviation derived from the replicate measurements of NGRIP samples and the replicate samples at YM85. Values of δ^{15}N and δ^{18}O at YM85 from 69.7 to 72.4 m (four levels) were rejected based on their anomalously high CO_2 concentrations. Those samples were contaminated by a leak through the sampling tube, which had been damaged and repaired before the sampling at these levels. We also rejected δ^{15}N and δ^{18}O values at two depths (12.1 and 44.0 m) at NGRIP, based on disagreement between δ^{15}N and δ^{18}O/2 by more than 3 standard deviations, and between duplicate measurements separated by a few months. Fractionation may have occurred during sample storage by selective adsorption on the inner surface or a small leak through the valves for those flasks.

2.2. Determination of the convective zone thickness

2.2.1. Barometric line fitting

Following previous studies, we use a linear regression of the measured isotopic profiles to determine the thickness of the convective zone [17]. In a static air column with uniform temperature, δ^{15}N and δ^{18}O/2 are proportional to depth with the barometric slope given by g/RT (‰ m^{-1}) (from Eq. (1)). The line should be fitted to data points below a certain depth where the isotopic profiles are not disturbed by seasonal thermal fractionation. Then, the depth intercept with zero isotopic enrichment (δ^{15}N=0) gives the thickness of the convective zone. This value is an average over a few decades, because the diffusion time from the surface to the deep firn is of this order. If there is no convective zone, the line intercepts at 0 m. The 13-m-thick convective zone at Vostok was calculated by line fitting to the data below 20 m [17]. We used only data below at least ~40 m because the seasonal thermal fractionation may extend to such depths [13]. For Dome Fuji, we excluded the deepest three data points based on the poor agreement between δ^{15}N and δ^{18}O.

Uncertainty reported below is the estimated 2σ error of the intercept from the scatter of the data and the error of each data point. Other uncertainties may arise if the gas does not reach the full barometric equilibrium in the deep firn, because of downward advection of firn air due to fast bubble trapping process (at very high-accumulation sites [19]) or temperature gradients in the deep firn due either to a geotherm (at very low-accumulation sites [7]) or to previous years' temperature variation (at sites with small convective zone, see result for NGRIP). These uncertainties are possibly up to 1–2 m for the sites studied here.

2.2.2. Diffusion model

We used the following equation as the governing equation for gas components in open pores of the bulk firn.

$$\frac{\partial \delta}{\partial t} = \frac{1}{s_o}\frac{\partial}{\partial z}\left(s_o D_{mol}(z,T,p)\left[\frac{\partial \delta}{\partial z} - \frac{\Delta m g}{RT} + \Omega \frac{\partial T}{\partial z}\right] + s_o D_{eddy}(z)\frac{\partial \delta}{\partial z}\right) + w(z)\frac{\partial \delta}{\partial z} \quad (2)$$

where δ is the isotopic delta value, s_o is open porosity, D_{mol} is effective molecular diffusivity tuned with CO_2 concentration data (our unpublished data measured at Tohoku University from 1999 to 2002), z is depth, T is temperature, p is pressure, Δm is mass difference between isotopes, g is gravitational acceleration, R is gas constant, D_{eddy} is eddy diffusivity, and w is descending speed of air due to bubble trapping. Based on results of theoretical models of wind pumping, the eddy diffusivity profile is assumed to exponentially decrease with depth [12]:

$$D_{eddy}(z) = D_{eddy,0}\exp\left(-\frac{z}{H}\right) \quad (3)$$

where $D_{eddy,0}$ is the eddy diffusivity at the surface and H is the e-folding depth. The vertical advection w is maximum at the lock-in depth, the same as the descending rate of the firn matrix, and decreases upwards with increasing porosity [20]. The model was run for $\delta^{15}N$ with $D_{eddy,0}$ ranging from 2×10^{-5} (comparable to the molecular diffusivity in free air) to 2×10^{-4} m^2 s^{-1} for each site except H72. The e-folding depth H is adjusted so that the model curves with the different $D_{eddy,0}$ agree with the data in deep firn. Temperature history observed by Automatic Weather Station ([21] for Antarctic sites, [22] for NGRIP) was used as a boundary condition. For Dome Fuji, a mean temperature gradient of +0.005 K/m due to the geotherm is assumed because of the low accumulation.

3. Results

3.1. Isotopic profiles

$\delta^{15}N$ and $\delta^{18}O$ at Dome Fuji, YM85, H72 and NGRIP increase with depth in most parts of the firn due to gravitational fractionation, as expected (Fig. 1). All the data for depths deeper than ~40 m follow the barometric slopes within the measurement uncertainties. Superimposed on the gravitational enrichment, a seasonal thermal fractionation signal is also evident as a positive anomaly in the shallow depths at Dome Fuji, YM85 and NGRIP, and a negative anomaly at H72, depending on the temperature gradient in the firn at the time of the samplings [13]. Due to the seasonal thermal signal, the convective zone is not obvious in the isotopic profiles. However, there is a significant offset between the data and the barometric line in the deep firn at YM85 and Dome Fuji (Fig. 1). In addition, the positive thermal anomaly in the shallow firn at these sites is much suppressed in comparison with the modeled curve without convective zone (Fig. 1, black curves) and in comparison with observations at sites lacking a deep convective zone [13]. These indicate the existence of thick convective zones at these sites. The data presented here show for the first time the superposition of the thermal signal and convection, which was not clear from the Vostok data [17].

In the lock-in zone at H72, YM85 and NGRIP, the isotopic ratios do not increase with time and depth, as expected. Unlike those sites, the Dome Fuji data continue to increase to the deepest sampling depth (104 m). This indicates that the Dome Fuji lock-in zone at present is less than a few meters thick given the sampling resolution (4 m). A thin lock-in zone has been recognized also at other low accumulation sites, Vostok and Dome C. The lack of preserved seasonal layering of snow at these sites may cause the absence of horizontally extensive impermeable layers, which are needed to lock-in the air. Also, the low accumulation rate may allow ample time for gases to diffuse even with a very low diffusivity.

3.2. Convective zone thickness

3.2.1. Line fitting method

We find from the line fitting method significant convective zones at Dome Fuji (8.6±2.6 m) and YM85 (14.0±1.8 m). These values are the mean of the thickness obtained from $\delta^{15}N$ and $\delta^{18}O$ (Fig. 1; Table 1), and the fitted lines are shown in Fig. 1. So far, a convective zone of similar magnitude has been found only at Vostok [17], which presumably has similar surface conditions as Dome Fuji (note however that a deep convective zone has been recently observed at the near-zero-accumulation Megadunes site [23]). All previously reported values at sites with higher temperature and accumulation rate than at Vostok or Dome Fuji have convective zones of only up to a few meters [16]. The thick convective zone at YM85 is therefore surprising because the temperature, accumulation rate and density profile are similar to those at NGRIP and are

Fig. 1. Depth profiles of $\delta^{15}N$ and $\delta^{18}O$ in the firn at (a) H72, (b) YM85, (c) Dome Fuji and (d) North GRIP. Also shown are barometric line, fitted line to the data with barometric slope, and model curves (see text). Measured temperature profile in the borehole after the firn air sampling is shown for NGRIP and YM85, as well as modeled temperature for all sites. Convective zone thickness with 2σ uncertainty is derived by the depth intercept of the fitted line with zero isotopic enrichment.

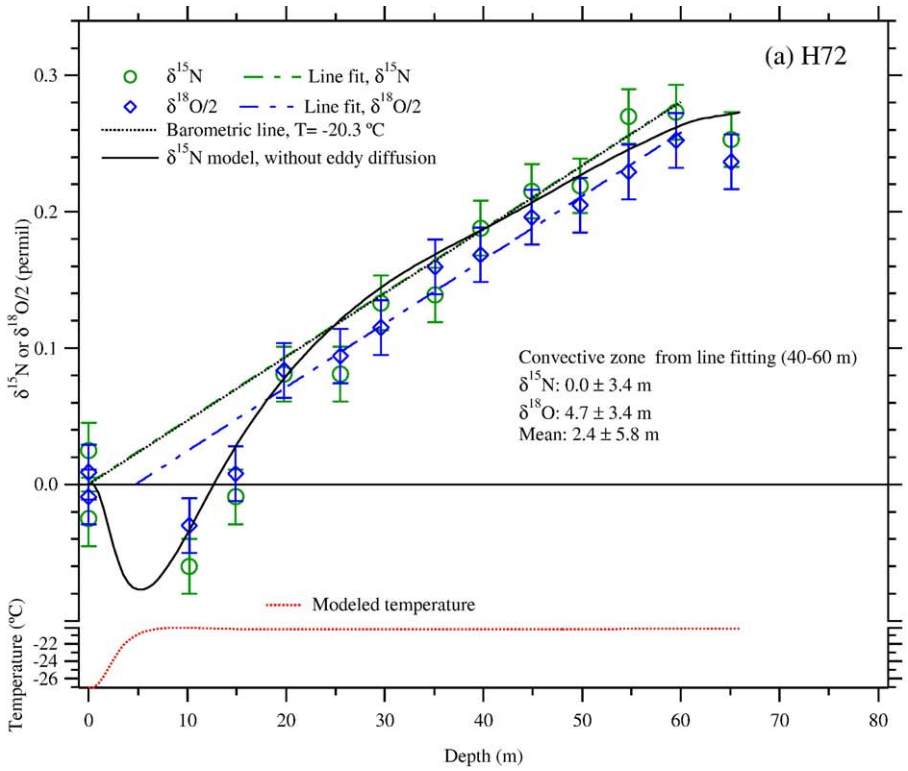
(a) H72
δ15N
δ18O/2
Line fit, δ15N
Line fit, δ18O/2
Barometric line, T= -20.3 ºC
δ15N model, without eddy diffusion
Convective zone from line fitting (40-60 m)
δ15N: 0.0 ± 3.4 m
δ18O: 4.7 ± 3.4 m
Mean: 2.4 ± 5.8 m
Modeled temperature
δ15N or δ18O/2 (permil)
Temperature (ºC)
Depth (m)

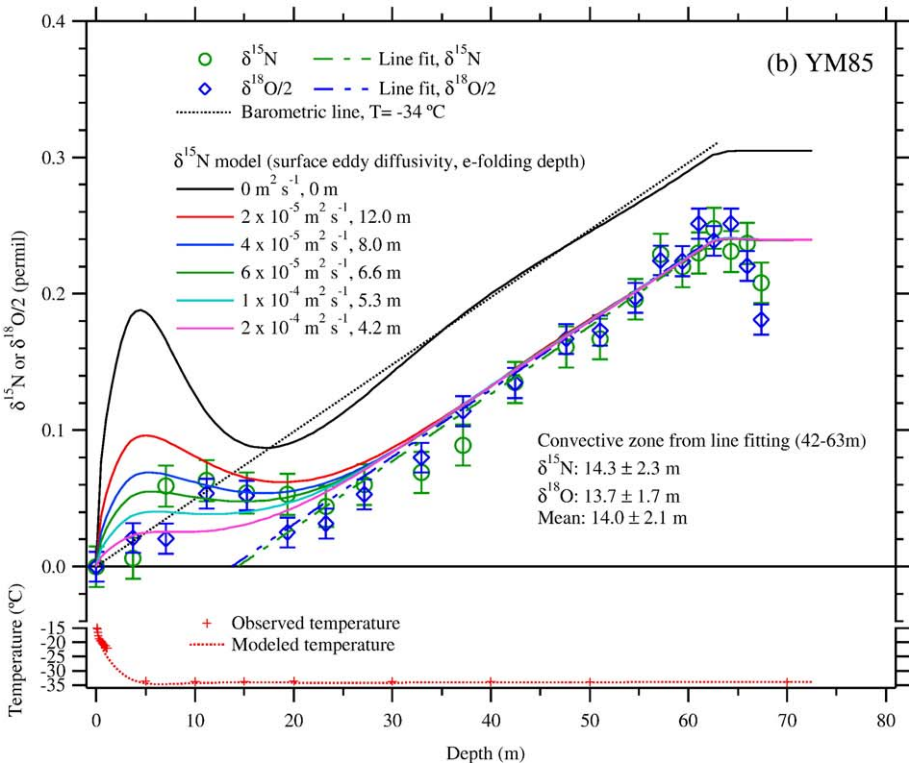
(b) YM85
δ15N
δ18O/2
Line fit, δ15N
Line fit, δ18O/2
Barometric line, T= -34 ºC
δ15N model (surface eddy diffusivity, e-folding depth)
0 m2 s-1, 0 m
2 x 10-5 m2 s-1, 12.0 m
4 x 10-5 m2 s-1, 8.0 m
6 x 10-5 m2 s-1, 6.6 m
1 x 10-4 m2 s-1, 5.3 m
2 x 10-4 m2 s-1, 4.2 m
Convective zone from line fitting (42-63m)
δ15N: 14.3 ± 2.3 m
δ18O: 13.7 ± 1.7 m
Mean: 14.0 ± 2.1 m
Observed temperature
Modeled temperature
δ15N or δ18O/2 (permil)
Temperature (ºC)
Depth (m)

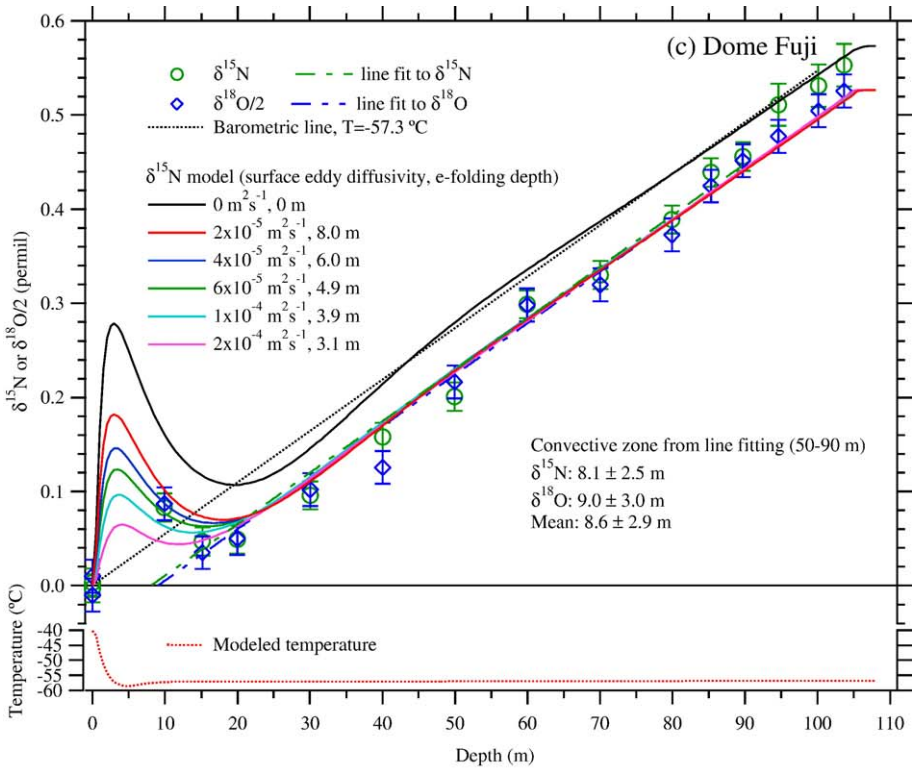

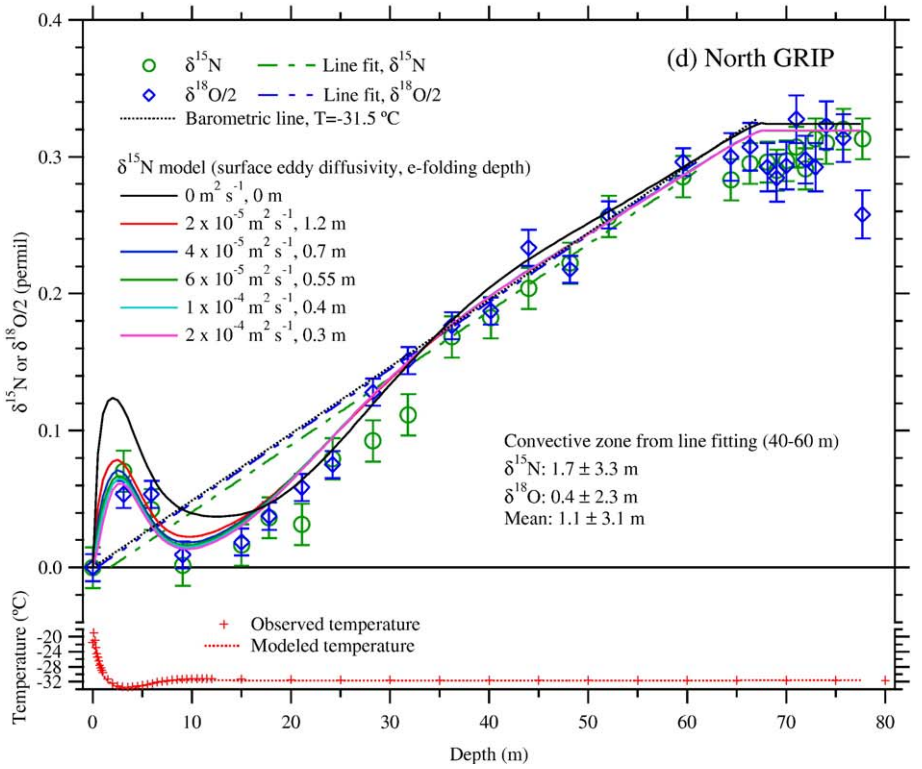

Fig. 1 (*continued*).

not at all extreme (Table 1). The existence of strong, steady katabatic winds at YM85 but not the other sites may provide an important clue (see below for discussion).

For H72 and NGRIP, the convective zone thickness is less than ~2 m. The small convective zone at NGRIP is consistent with the independent estimate by Landis et al. [16] using samples from a different borehole during the same period. However, it is not clear whether weak convection occurs at these sites, because the results are not significantly different from zero. At NGRIP, a significant negative anomaly relative to the regression lines is evident at ~10 to 30 m, unlike YM85 and Dome Fuji. This is created by thermal diffusion in the previous winter and subsequent downward propagation by molecular diffusion. This also indicates that the convective zone is small at this site.

3.2.2. Model fitting method

For YM85 and Dome Fuji, the model creates distinctive isotopic profiles in shallow firn with different eddy diffusivity profiles (Fig. 1). At YM85, a good match to data is obtained with the surface diffusivity ranging from 4×10^{-5} to 1×10^{-4} m^2 s^{-1} and the according e-folding depth ranging from 8.5 to 5.6 m. At Dome Fuji, surface diffusivities ranging from 4×10^{-5} to 1×10^{-4} m^2 s^{-1} and e-folding depths of 7.0–4.4 m produce acceptable fits. The surface eddy diffusivities at these sites are several times greater than the molecular diffusivity. More precise comparison between the data and model requires higher sampling resolution in the shallow firn as well as more precise measurement. Sampling in different seasons would also help understand possible seasonality of convection (e.g. by buoyancy-driven convection in winter).

For NGRIP, the fit between the $\delta^{15}N$ data and model curves in the shallow firn (<~15 m) is much better with eddy diffusion than without, indicating that weak convection does occur at this site. Unlike YM85 and Dome Fuji, the model curves are too close to usefully constrain the eddy diffusivity. The model curve without eddy diffusion for H72 generally fits the $\delta^{15}N$ data within the data uncertainty. The modeled slope below ~40 m is significantly smaller than the barometric slope, probably due to advection by bubble formation, though the data uncertainty is too large to confirm it.

The eddy diffusivity profiles are compared with molecular diffusivity profiles for YM85, Dome Fuji and NGRIP (Fig. 2) in order to derive an alternative expression of the convective zone thickness. We expect that the crossover from eddy diffusion to molecular diffusion as the dominant mechanism for gas movement occurs deepest at YM85 and shallowest at NGRIP, from the estimated convective zone thickness by the line fitting method. Indeed, the crossover occurs at 7±2, 11±2, and 0.5±0.5 m at Dome Fuji, YM85, and NGRIP, respectively (Fig. 2, Table 1). Here the errors are estimated based on the results using different eddy diffusivity profiles and an uncertainty in the molecular diffusivity (arbitrarily assumed to be ±20%). These crossover depths are comparable within error to the convective zone thickness estimated by the line fitting method.

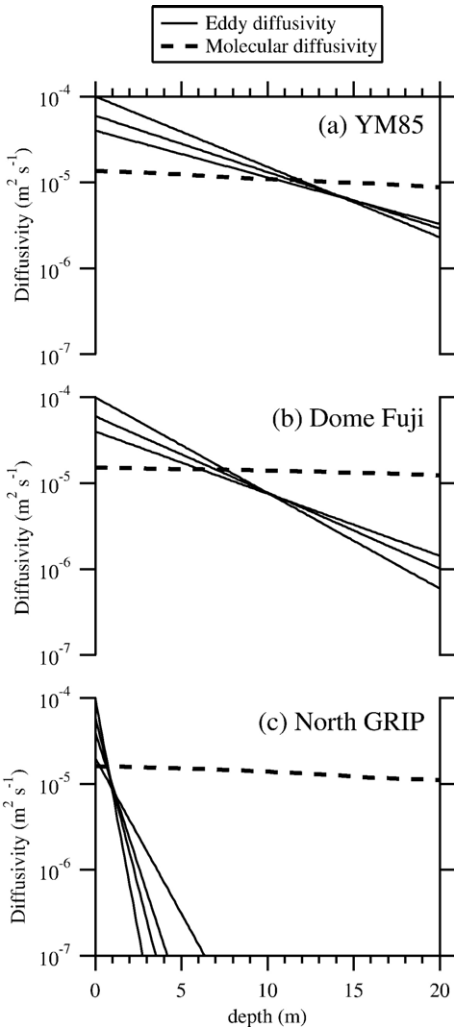

Fig. 2. Comparison between effective molecular diffusivity and eddy diffusivity at (a) YM85, (b) Dome Fuji and (c) NGRIP. The molecular diffusivity is corrected for temperature, atmospheric pressure, and firn porosity at the sites. The eddy diffusivity profile is tuned so that the modeled isotopic profile agrees with the data. Several lines for each site represent the range of possible eddy diffusivity profiles.

4. Discussion

We discuss here how glaciological and meteorological conditions such as porosity, accumulation rate, and wind speed can cause the differences in the convective zone among the studied sites. Vertical air flow in the firn may be described by Darcy's Law:

$$q = \frac{k}{\mu}\frac{\mathrm{d}p}{\mathrm{d}z} \tag{4}$$

where q is volumetric flow rate (positive downward), k is intrinsic permeability, μ is viscosity of air, and p is pressure [12]. All three terms in principle may vary from site to site and contribute to the observed differences. We show here that the thick convective zones at Dome Fuji and YM85 may be ascribed to the proximate causes of high permeability near the surface and stronger forcing of convection (pressure gradient), respectively, as follows.

The permeability of the firn is influenced by porosity, the variance of porosity, and the size and shape of individual pores [24]. High porosity, uniform porosity, and large individual pores are expected to result in large permeability. Dome Fuji seems to meet these conditions. The porosity at the surface is largest and the accumulation rate is lowest among the four sites. A given firn parcel spends ~50 yrs in the top 4 m of firn at Dome Fuji, in contrast to 6–12 yrs at the other sites. The longer exposure to solar radiation and the large seasonal temperature gradient is expected to enlarge pore diameter, through grain growth and formation of depth hoar. Also, the mean vertical length of pores at Dome Fuji is longer than the horizontal length by 10–20% due to depth hoar formation (J. Okuyama, pers. comn., 2005). This could also help air to flow vertically, which is key to convective mixing. If the vertical density profile fluctuates around the mean due for example to seasonality of snowfall, high-density layers may impede vertical airflow. This is not the case for Dome Fuji, where the low accumulation rate results in the destruction of most horizontally continuous layering due to reworking and redeposition of snow. Although layered structures such as crusts are observed in the Dome Fuji core, their horizontal extension is probably small.

The low air viscosity at Dome Fuji (Table 1) is consistent with the thick convective zone at this site, but it is unlikely to be a major factor controlling the convective zone thickness because viscosity varies among the sites by only ~10%. Also it does not explain the large convective zone at YM85.

At YM 85, the temperature and accumulation rate are similar to those at NGRIP, and the surface porosity is lowest among the four sites. The relatively thick lock-in zone at this site suggests that there are seasonal high-density layers, which would hamper vertical airflow in shallow firn. Thus the permeability in the firn is unlikely to be particularly large. Consequently, we suspect that the very thick convective zone at YM85 may be ascribed to the pressure gradient that forces airflow in the firn. Strong wind, together with surface topography, may create pressure gradients large enough to cause convection in the firn (wind pumping) [12]. Indeed YM85 is located in a strong katabatic wind region and the mean wind speed is ~12 m s^{-1}, in contrast to ~4 m s^{-1} at NGRIP (Table 1). Therefore, this may be the first observation of a deep convective zone created by wind pumping.

Other factors may affect convective zone thickness. The magnitude of the molecular diffusivity, which varies inversely with barometric pressure, should affect the convective zone thickness, because the convective zone is determined by the relative magnitudes of eddy and molecular diffusivity. If we compare YM85 and NGRIP, which have similar temperature but different elevation, the lower elevation of YM85 (thus smaller molecular diffusivity) should therefore slightly decrease the importance of molecular diffusion as a vertical transport mechanism. Bernard or buoyancy-driven convection may be important during winter when firn is warmer than the atmosphere [13]. If this is the case, its contribution should be largest at Dome Fuji due to the large amplitude of seasonal temperature variation.

Unfortunately, a simple relationship between surface conditions and the convective zone is not implied by these results. The mean wind speed at Dome Fuji is only 2 m s^{-1}, but the convective zone is significant probably due to high permeability. On the contrary, H72 has relatively high wind speed of 8 m s^{-1} but the convective zone is only 2 m. High accumulation at H72 may create and preserve thicker high-density layers than at the other sites, which prevent vertical airflow. An alternative speculation is that average wind speed may be less important for the convective zone than the wind velocity distribution. The wind speed and direction are probably more variable at H72 than YM85 because of its proximity to the coast. Variable wind may not create a persistent pressure gradient in the firn to establish a deep convective zone. The difference between YM85 and H72 suggests the hypothesis that thick convective zone from strong wind forcing may only occur in middle-elevation sites in Antarctica where the katabatic wind is very strong and quasi-unidirectional. The convective zone at Dome C is only a few meters [16] despite the fact

that the site is characterized by similar surface condition as Dome Fuji and Vostok. Because the wind would not be the factor controlling the convective zone thickness at these high-elevation sites, the horizontal layering of the shallow firn as well as other physical properties probably are responsible for the difference.

5. Conclusions

Four polar sites with varying accumulation rate, wind, elevation, and temperature are investigated to elucidate possible relationships between deep air convection in the firn and environmental variables. The motivation for this study is to better understand deep ice core records of trapped gases, in which past occurrence of convective zones may reduce the magnitude of observed trapped gas fractionation. An overall relationship between low accumulation rate and the presence of deep convective zones is suggested by our data, with one notable exception that may be explained by strong wind forcing of air movement through the firn. However, the controls on convective zone thickness do not appear to be simple and probably include the degree of horizontal layering of shallow firn properties as well as other shallow firn structural elements.

The largest observed convective zone of 14 m is still only about half of the current inconsistency implied from the deep ice cores. Another search for a deep convective zone is ongoing using firn air from a near-zero-accumulation site [23]. However, these results are still unlikely to fully explain the inconsistency between deep ice core gas isotopes and firn densification models.

Acknowledgements

We thank Tomomi Yamada of Hokkaido University, Keisuke Suzuki of Shinshu University for the sample collection at H72 and Dome Fuji, Morimasa Takata of Nagaoka University of Technology for assistance for the sample collection at North GRIP, and Jakob Schwander of University of Bern for firn temperature measurement as well as collaboration at North GRIP. The 39th and 42nd Japanese Antarctic Research Expedition and North GRIP 2001 field participants made substantial support for the drilling and sample collection. We thank Shuhei Takahashi of Kitami Institute of Technology for providing Antarctic AWS data, and Konrad Steffen for providing NGRIP AWS data. Takao Kameda of Kitami Institute of Technology and two anonymous reviewers made valuable comments. Funding for K.K. during modeling and writing was provided by NSF grants OPP02-30452 (to J.S.) and a Gary Comer Abrupt Climate Change Fellowship.

References

[1] J.R. Petit, J. Jouzel, D. Raynaud, N.I. Barkov, J.-M. Barmola, I. Basile, M. Bender, J. Chapppellaz, M. Davis, G. Delaygue, M. Demotte, V.M. Kotlyakov, M. Legrand, V.Y. Lipenkov, C. Lorius, L. Pepin, C. Ritz, E. Saltzman, M. Stievenard, Climate and atmospheric history of the past 420000 years from the Vostok ice core, Antarctica, Nature 399 (1999) 429–436.

[2] EPICA Community Members, Eight glacial cycles from an Antarctic ice core, Nature 429 (2004) 623–628.

[3] K. Kawamura, T. Nakazawa, S. Aoki, S. Sugawara, Y. Fujii, O. Watanabe, Atmospheric CO_2 variations over the last three glacial–interglacial climatic cycles deduced from the Dome Fuji deep ice core, Antarctica using a wet extraction technique, Tellus 55B (2003) 126–137.

[4] O. Watanabe, J. Jouzel, S. Johnsen, F. Parrenin, H. Shoji, N. Yoshida, Homogeneous climate variability across East Antarctica over the past three glacial cycles, Nature 422 (2003) 509–512.

[5] J. Schwander, J.M. Barnola, C. Andrie, M. Leuenberger, A. Ludin, D. Raynaud, B. Stauffer, The age of the air in the firn and the ice at Summit, Greenland, J. Geophys. Res. 98 (1993) 2831–2838.

[6] N. Caillon, J.P. Severinghaus, J. Jouzel, J.M. Barnola, J.C. Kang, V.Y. Lipenkov, Timing of atmospheric CO_2 and Antarctic temperature changes across termination III, Science 299 (2003) 1728–1731.

[7] C. Goujon, J.M. Barnola, C. Ritz, Modeling the densification of polar firn including heat diffusion: application to close-off characteristics and gas isotopic fractionation for Antarctica and Greenland sites, J. Geophys. Res. 108 (2003) art. no.-4792.

[8] T. Sowers, M. Bender, D. Raynaud, Y.S. Korotkevich, $\delta^{15}N$ of N_2 in air trapped in polar ice: a tracer of gas transport in the firn and a possible constraint on ice age–gas age differences, J. Geophys. Res. 97 (1992) 15683–15697.

[9] K. Kawamura, Variations of Atmospheric Components Over The Past 340,000 Years from Dome Fuji deep ice core, Antarctica, Ph.D. Tohoku University, 2000.

[10] J.P. Severinghaus, A. Grachev, B. Luz, N. Caillon, A method for precise measurement of argon 40/36 and krypton/argon ratios in trapped air in polar ice with applications to past firn thickness and abrupt climate change in Greenland and at Siple Dome, Antarctica, Geochim. Cosmochim. Acta 67 (2003) 325–343.

[11] J.P. Severinghaus, T. Sowers, E.J. Brook, R.B. Alley, M.L. Bender, Timing of abrupt climate change at the end of the Younger Dryas interval from thermally fractionated gases in polar ice, Nature 391 (1998) 141–146.

[12] S.C. Colbeck, Air movement in snow due to windpumping, J. Glaciol. 35 (1989) 209–213.

[13] J.P. Severinghaus, A. Grachev, M. Battle, Thermal fractionation of air in polar firn by seasonal temperature gradients, Geochem. Geophys. Geosyst. 2 (2001) art. no.-2000GC000146.

[14] H. Craig, Y. Horibe, T. Sowers, Gravitational separation of gases and isotopes in polar ice caps, Science 242 (1988) 1675–1678.

[15] T. Blunier, J. Schwander, J. Chappellaz, F. Parrenin, J.M. Barnola, What was the surface temperature in central Antarctica during the last glacial maximum? Earth Planet. Sci. Lett. 218 (2004) 379–388.

[16] A. Landais, J.-M. Barnola, K. Kawamura, N. Caillon, M. Delmotte, T. van Ommen, G. Dreyfuss, J. Jouzel, V. Masson-Delmotte, B. Minster, J. Freitag, M. Leuenberger, J. Schwander, B. Huber, D. Etheridge, V. Morgan, Firn-air $\delta^{15}N$ in modern polar sites and glacial–interglacial ice: a model-data mismatch during glacial periods in Antarctica? Quat. Sci. Rev. 25 (2005) 49–62.

[17] M. Bender, T. Sowers, J.M. Barnola, J. Chappellaz, Changes in the O_2/N_2 ratio of the atmosphere during recent decades reflected in the composition of air in the firn at Vostok Station, Antarctica, Geophys. Res. Lett. 21 (1994) 189–192.

[18] T. Sowers, M. Bender, D. Raynaud, Elemental and isotopic composition of occluded O_2 and N_2 in polar ice, J. Geophys. Res. 94 (1989) 5137–5150.

[19] C.M. Trudinger, I.G. Enting, D.M. Etheridge, R.J. Francey, V.A. Levchenko, L.P. Steele, D. Raynaud, L. Arnaud, Modeling air movement and bubble trapping in firn, J. Geophys. Res. 102 (1997) 6747–6763.

[20] S. Sugawara, K. Kawamura, S. Aoki, T. Nakazawa, G. Hashida, Reconstruction of past variations of $\delta^{13}C$ in atmospheric CO_2 from its vertical distribution observed in the firn at Dome Fuji, Antarctica, Tellus 55B (2003) 159–169.

[21] S. Takahashi, T. Kameda, H. Enomoto, H. Motoyama, O. Watanabe, Automatic Weather Station (AWS) data collected by the 33rd to 42nd Japanese Antarctic Research Expedition during 1993–2001, JARE Data Report 276 (Meteorology 36), 2004, p. 416.

[22] K. Steffen, J. Box, Surface climatology of the Greenland ice sheet: Greenland climate network 1995–1999, J. Geophys. Res. 106 (2001) 33951–33964.

[23] J.P. Severinghaus, M. Fahnestock, M. Albert, T. Scambos, C. Shuman, Do deep convective zones exist in low-accumulation firn? Eos Trans. AGU 85 (47) (2004) Fall Meet. Suppl., Abstract C31C-07.

[24] M.R. Albert, E.F. Shultz, F.E. Perron Jr., Snow and firn permeability at Siple Dome, Antarctica, Ann. Glaciol. 31 (2000) 353–356.

[25] F. Nishio, T. Furukawa, G. Hashida, M. Igarashi, T. Kameda, M. Kohno, H. Motoyama, K. Naoki, K. Satow, K. Suzuki, M. Takata, Y. Toyama, T. Yamada, O. Watanabe, Annual-layer determinations and 167 year records of past climate of H72 ice core in east Dronning Maud Land, Antartica, Ann. Glaciol. 35 (2002) 471–479.

[26] North Greenland Ice Core Project Members, High-resolution record of Northern Hemisphere climate extending into the last interglacial period, Nature 431 (2004) 147–151.